metals

MDPI

Article

Sustainable Recovery of Secondary and Critical Raw Materials from Classified Mining Residues Using Mycorrhizal-Assisted Phytoextraction

Adalgisa Scotti [1,2,*], Stefano Milia [2], Vanesa Silvani [3], Giovanna Cappai [2,4], Daniela Guglietta [2], Francesca Trapasso [2], Emanuela Tempesta [2], Daniele Passeri [2], Alicia Godeas [3], Martín Gómez [1] and Stefano Ubaldini [2]

[1] Bio Environmental Laboratory, International Center for Earth Sciences, National Atomic Energy Commission, San Rafael Mendoza 5600, Argentina; mpgomez@cnea.gov.ar
[2] Institute of Environmental Geology and Geoengineering, National Research Council of Italy, Research Area of Rome 1, 00185 Montelibretti, Italy; stefano.milia@igag.cnr.it (S.M.); gcappai@unica.it (G.C.); danielaguglietta@gmail.com (D.G.); francesca.trapasso@igag.cnr.it (F.T.); emanuela.tempesta@igag.cnr.it (E.T.); daniele.passeri@igag.cnr.it (D.P.); stefano.ubaldini@igag.cnr.it (S.U.)
[3] Faculty of Exact and Natural Science, Institute of Biodiversity and Applied and Experimental Biology, National Scientific and Technical Research Council—University of Buenos Aires, Buenos Aires 1428, Argentina; vsilvani@bg.fcen.uba.ar (V.S.); godeas@bg.fcen.uba.ar (A.G.)
[4] Department of Civil-Environmental Engineering and Architecture, University of Cagliari, 09123 Cagliari, Italy
* Correspondence: scotti@cnea.gov.ar

Citation: Scotti, A.; Milia, S.; Silvani, V.; Cappai, G.; Guglietta, D.; Trapasso, F.; Tempesta, E.; Passeri, D.; Godeas, A.; Gómez, M.; Ubaldini, S. Sustainable Recovery of Secondary and Critical Raw Materials from Classified Mining Residues Using Mycorrhizal-Assisted Phytoextraction. *Metals* **2021**, *11*, 1163. https://doi.org/10.3390/met11081163

Academic Editor: Fernando Castro

Received: 21 June 2021
Accepted: 20 July 2021
Published: 22 July 2021

Abstract: In this work, mycorrhizal-assisted phytoextraction (MAP, *Helianthus annuus*–arbuscular mycorrhizal fungus *Rhizophagus intraradices*–Zn-volcanic ashes) was applied for the recovery of secondary and critical raw materials (SRMs and CRMs, respectively) from Joda West (Odisha, India) mine residues, within a novel multidisciplinary management strategy. Mine residues were preliminarily characterized by using advanced analytical techniques, and subsequently mapped, classified and selected using multispectral satellite Sentinel-2A images and cluster analysis. Selected mine residues were treated by MAP at laboratory scale, and the fate of several SRMs (e.g., Zn, Cr, As, Ni, Cu, Ca, Al, K, S, Rb, Fe, Mn) and CRMs (such as Ga, Ti, P, Ba and Sr) was investigated. Bioconcentration factors in shoots (BC_S) and roots (BC_R) and translocation factors (TF) were: 5.34(P) > BCS > 0.00(Al); 15.0(S) > BCR > 0.038(Ba); 9.28(Rb) > TF > 0.02(Ti). Results were used to predict MAP performance at larger scale, simulating a Vegetable Depuration Module (VDM) containing mine residues (1 m^3). Estimated bio-extracting potential (BP) was in the range 2417 g/m^3 (K) > BP> 0.14 g/m^3 (As), suggesting the eventual subsequent recovery of SRMs and CRMs by hydrometallurgical techniques, with final purification by selective electrodeposition, as a viable and cost-effective option. The results are promising for MAP application at larger scale, within a circular economy-based approach.

Keywords: hydrometallurgy; resource recovery; mycorrhizal-assisted phytoremediation; remote sensing; circular economy

1. Introduction

A successful economy minimizes the production of waste and reuses it as a raw material. Resource constraints and environmental pressures will accelerate the transition from a linear "extraction-use-throw away" model of production and consumption to a circular one: moving towards a near-zero waste society has an environmental rationale and it represents a factor of competitiveness at the same time [1].

An integrated multidisciplinary approach for characterization and analysis of iron- and manganese-rich mine residues in Joda West (State of Odisha, India), and their valorization as a resource, was recently proposed by Guglietta et al. [1]. Such an approach would simultaneously promote both economic development and environmental protection. Moreover, the integration of different expertise from characterization to exploitation, passing through mining, reusing and monitoring, will consolidate the knowledge of the various processes. The application of innovative integrated technologies is urgently necessary to create synergistic efforts and results for sustainable exploitation of mining residues. The aim is to promote the transition to a more circular model that can strongly contribute, with products, processes and business models that are designed, to maximize the value and utility of resources while at the same time reducing adverse health and environmental impacts (Figure 1). In particular, this multidisciplinary strategy combines:

1. New sensitive technologies (such as remote sensing technologies) for mapping and classification of mining wastes containing minerals and metals;
2. New solutions for chemical, physical and morphological characterization;
3. An eco-innovative methodology for converting mining waste into resource: mycorrhizal-assisted phytoextraction (MAP) of mining wastes, and the consequent accumulation of secondary and critical raw materials (SRMs and CRMs, respectively) in biomass tissues;
4. Recovery of SRMs and CRMs from biomass through hydrometallurgy and/or electrochemical methods. The leaching extraction is selective and allows the recovery of all the contained elements because specific reagents are used for each of them, applying innovative processes (e.g., thiourea process, thiosulfate process, etc.). The metals are purified to a high degree of purity by electrochemical methods.

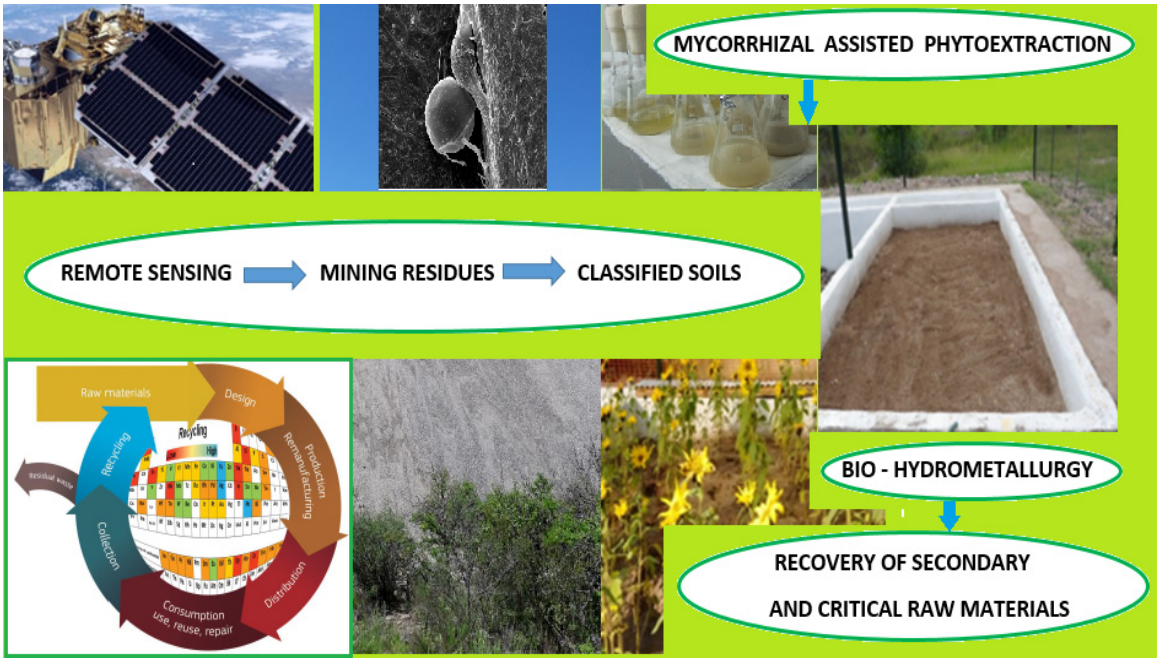

Figure 1. A scheme of the proposed multidisciplinary strategy for classification and recovery of secondary and critical raw materials (Adapted from ref. [2]).

The synergy between points 1 and 3 is of particular interest, since it couples low-cost, highly efficient remote sensing and bioremediation technologies. As to remote sensing classification (i.e., point 1), it highlighted mining deposits rich in Fe and Mn in a mine area and all different data were stored in a geodatabase [1], which is a powerful tool for mine waste management and for the selection of samples containing valuable minerals and

metals to treat by phytoremediation technique. As to phytoremediation, it is widely recognized as an environmentally friendly technique that uses plants and beneficial microorganisms to remove pollution at greatly reduced costs and minimum adverse side effects [3]. Regarding the bioaccumulation of SRMs by using metal hyperaccumulator plants, it was widely reported that *Helianthus annuus* (Asteraceae family) can accumulate large amounts of Ni, Mn, Zn, Cu, Pb, As, and Cd [4–6] and CRMs such as Ga, Sr, Ti [1,7,8]. This capacity of accumulation in their biomass can be enhanced by association in their roots with the arbuscular mycorrhizal (AM) fungi belonging to the Phylum Glomeromycota [9]. In this mycorrhizal association, plants benefit from nutritional supply and growth improvement, and it also play a key role in stress alleviation, such as that imposed by excess heavy metals [10]. Some mechanisms responsible for the amelioration of toxicity in the host plants mediated by the AM fungi are known, such as sequestration and accumulation of different metals by extra- and intra-radical AM fungal structures (spores, mycelia, vesicles), and the modulation of genetic expression in the detoxification process of plants [10,11]. The AM symbiosis is frequently included in the bioremediation strategies of different metal polluted soils [4,12]. Various reports have shown that the AM association established between sunflowers (*Helianthus annuus* L.) and the AM fungus *Rhizophagus intraradices* is effective for the uptake and accumulation of various chemical elements [4,13]. During the bioremediation process, the elements bioaccumulated in plant biomass can also be subsequently recovered and reused. However, little is known about phytoaccumulation of certain CRMs and SRMs by using mycorrhizal sunflower plants when grown in contaminated soils. In previous works, we found significant accumulation of SRMs (i.e., Zn, Mn, Cu) and a CRM (i.e., Sr) from contaminated soil by using the MAP system comprised of "*H. annuus*–*R. intraradices*–Zn 350-volcanic ash" [1,14,15] at laboratory scale. However, some raw materials have not yet been investigated at a larger scale approach. The synergistic coexistence of soil, water, plants, and soil microorganisms has been also exploited in constructed wetlands, which imitate the hydrological system of natural wetlands and have become a simple, low-cost alternative for wastewater treatment [16–18]. The MAP system introduced into an innovative constructed wetland called Vegetable Depuration Module (VDM) [8] was proposed as a scaling tool to reach a technology readiness level (TRL) 6 (i.e., pilot test) by simulation of a relevant environment characterized by high concentrations of chemical elements [19]. Using this VDM, the first cycle of an engineered process for decontamination of a polluted environment composed of wastewater and substrate (soil) with an excess of chemical elements can be simulated and tested. In this study, the outcomes of spectral and mineralogical characterization of mine residues, and their mapping and classification by remote sensing technologies were used for the selection of samples rich in Fe and Mn. The selected mining residues were treated at lab-scale (TRL-2) with the MAP system (*H. annuus*–*R. intraradices*–Zn 350-volcanic ash) for the recovery of several SRMs (i.e., Fe, Mn, Zn, Cr, As, Ni, Cu, Rb, Al, K, S, Ca) and CRMs (i.e., Ba, Ga, P, Ti and Sr) from plant biomass. With a future perspective of on-site treatment of Joda West mine residues (TRL-6), results achieved at TRL-2 were used to estimate the bioextracting potential of the MAP system in the VDM, specifically focusing on less studied SRMs and CRMs.

2. Materials and Methods

2.1. Fe and Mn Mine Wastes

The Fe and Mn mine area is located in the village of Joda, in the Keonjhar district of Odisha (India) (Figure 2). In situ sampling campaign was carried out on November 29th in 2017 by scientific and technical staff of the Institute of Environmental Geology and Geoengineering (National Research Council, CNR, Italy) in collaboration with TATA Steel and the National Environmental Engineering Research Institute (NEERI-India). Thirty-six different samples were collected from waste, stock deposits and dumps. For each sample, additional information consisting of GPS coordinate, pictures and a brief description of

the sampling area were gathered. Furthermore, for each sample about 200 g were selected for further laboratory analysis (chemical, physical and spectral analysis), and remote sensing analysis at National Research Council (CNR) in Italy.

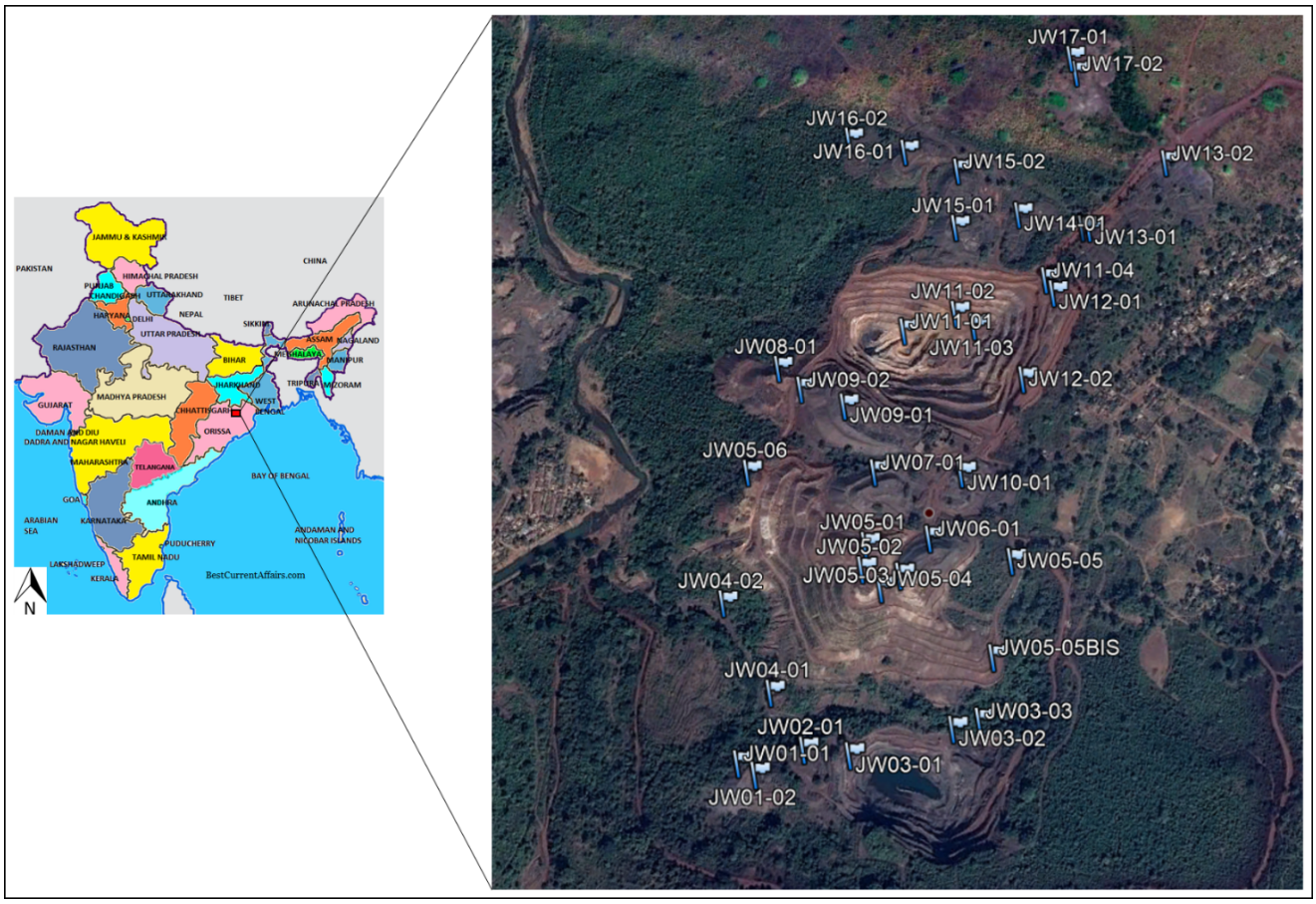

Figure 2. Location of the study area and in situ sampling campaign overlaid on Sentinel-2A image acquired on 29 November 2017.

2.2. The Joda West Iron and Manganese Mine Geodatabase

For each sample collected in the mining area, the corresponding spectral signature was extracted by the image and the different spectral classes were individuated by means of the interpretation of chemical and mineralogical analysis. Afterwards, the map of Fe and Mn residues was obtained by applying supervised pixel based classification and the algorithm used in this methodology was Spectral Angle Mapper (SAM) [1]. The Sentinel-2A map highlighted residue deposit areas with different mean percentages of Fe and Mn (Figure 3) as well as their surface alteration (i.e., presence of vegetation). In particular, Class 1 was characterized by presence of sparse vegetation that indicated residues accumulated over a long period; Class 2 was represented by a steady accumulation of extractive residues; Class 3 showed high percentages of Fe and Mn, but these residues were not of interest for the steel industry as they would need prior ore dressing; Class 4 contained residues with lower Fe and Mn content. For the phytoremediation process, Class 2 and Class 4 residue samples have been selected and analyzed.

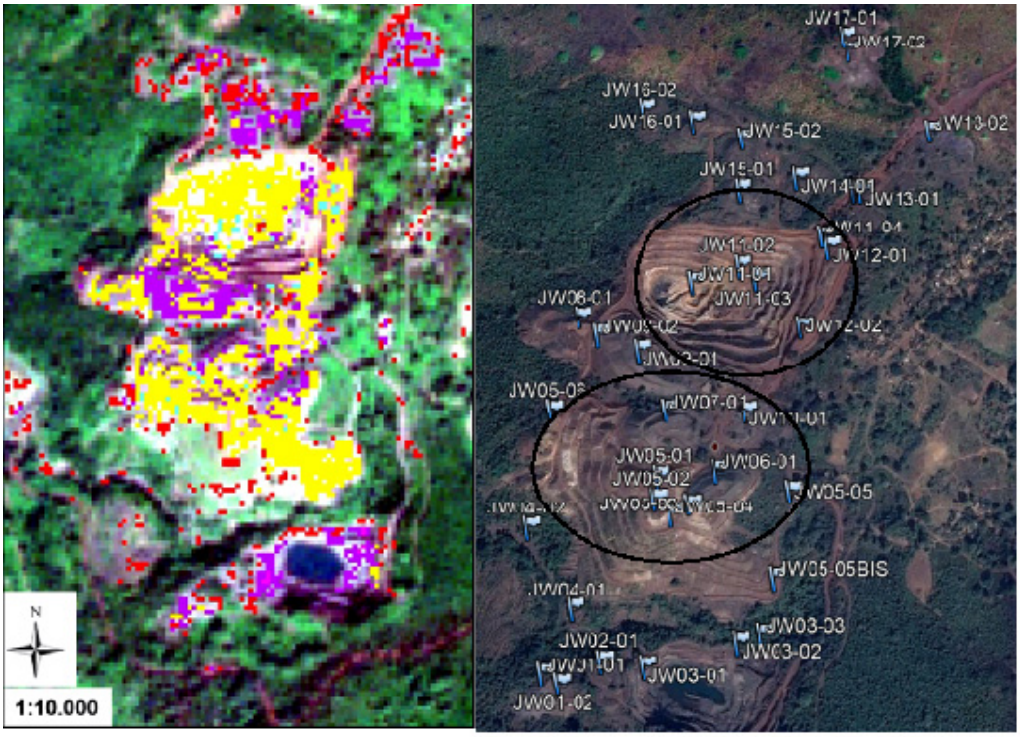

		Fe mean %	Mn mean %	Si mean %	Al mean %
CLASS 1		34.27	11.33	7.41	5.27
CLASS 2		38.44	10.29	5.31	4.11
CLASS 3		31.28	24.70	3.60	2.89
CLASS 4		5.38	0.62	30.61	9.27

Figure 3. Spatial distribution of the mining residue classes (**left**) and samples overlaid (**right**) on Sentinel-2A image. Black circles indicate the areas of soil selected for MAP.

The in situ observations and the results of statistical, spectral, chemical and mineralogical analysis as well as of the satellite classification process were collected into a geodatabase to identify the mining residues stored in old dumps or fresh landfills in the Joda West mine. The following information was recorded for each sample: location (including coordinates); details of the study site (including land cover, land use, geomorphology); information and observations on the residue (including results of analysis, pictures, color, and area if known). The Joda West geodatabase was built using ESRI's ArcGIS 10.2 software (Keonjhar district, State of Odisha, India). The geodatabase is useful for progressively identifying the residue areas of spatial importance for optimized management, as well as for highlighting the mining residues rich in Fe and Mn that could be potentially used for bioremediation processes. In order to provide a useful tool for researchers as well as decision makers (stakeholders), the GIS layers were exported and reassembled as a project file in Google Earth. The final Joda West project file is in a Google Earth KMZ (keyhole Markup Language—zipped) format (Figure 4).

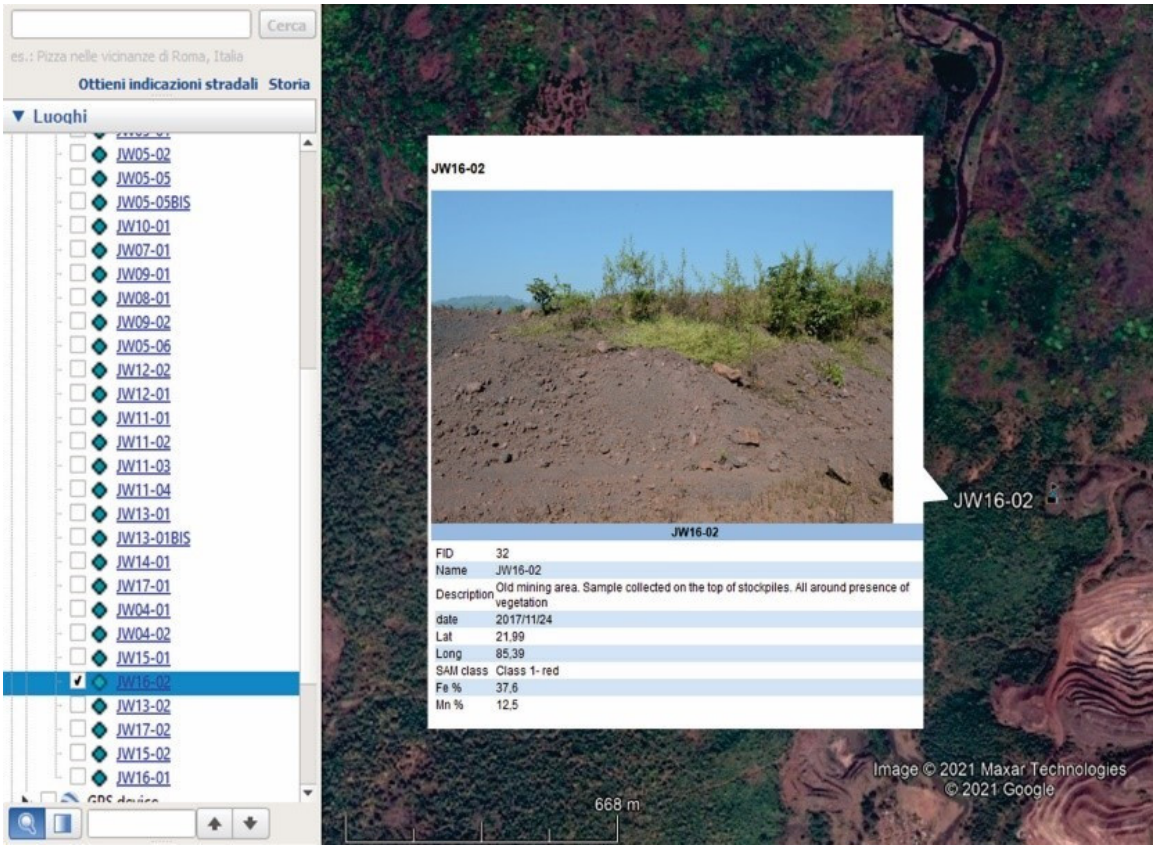

Figure 4. Example of the Joda West geodatabase: JW 16-02 sample.

2.3. MAP Test at TRL-2 Scale

2.3.1. Plant Material and AM Fungal Strain

The MAP system consisted of sunflowers (*Helianthus annuus L.*, hybrid cultivar DK4045, Syngenta seeds) colonized by the AM fungus *Rhizophagus intraradices* strain GA5 (provided by Bank of Glomeromycota In Vitro, Faculty of Exact and Natural Sciences, Buenos Aires University, www.bgiv.com.ar, accessed on 21 July 2021) grown in a substrate comprised of a homogeneous mixture of soil and volcanic ash (50:50, *v*/*v*) and supplemented with $ZnSO_4$ (as catalyst compound) [8]. The AM fungal strain was propagated using transformed carrot roots grown in minimal medium as described by Silvani et al. [20]. This fungal strain was previously reported to promote tolerance to different abiotic stresses in several plant species and to have potential as bioremediator [8,21].

2.3.2. TRL-2 Experimental Setup

Fe- and Mn-rich soil samples classified as Class 2 and 4 by Sentinel-2A remote sensing were used to test the MAP system at TRL-2 scale. For that purpose, homogeneous composite soil samples (CS) were prepared by mixing individual samples from selected areas of the Indian mine. The volcanic ash (VA) and granular pumice stone (PS) (diameter, 3–6 mm) were provided by Pumex S.P.A. (Lipari Island, Italy) and Europomice S.R.L. (Milan, Italy), respectively. The fertile commercial topsoil (FCT) was provided by Euroterriflora S.R.L. (Bucine, Italy). The physical-chemical properties and mineralogical characterization of CS, VA and FCT are described in Guglietta et al. [1]. To corroborate that non-indigenous AM fungal propagules were present in the mine soil samples and the commercial topsoil, a subsample (10 g) of each type of soil was wet sieved and decanted and then checked for AM fungal spores under a binocular microscope. Before planting, sunflower seeds were surface-sterilized with an ethanol solution (70%, *v*/*v*) and washed twice

in sterile water. The experimental design of the TRL-2 system consisted of 16 pots (height: 12 cm; diameter: 13.5 cm), as detailed below:

- $MA_{1–4}^{+}$. Four pots filled with CS and VA in a 1:1 (*v*/*v*) ratio, completing to 500 mL and 125 mL granular PS. Considering the CS only, 300–500 ppm $ZnSO_4$ were added. At least three sunflower seeds were sown and inoculated with a piece of 4-month old monoxenic culture (containing approximately 300 spores, mycelia and colonized roots).
- $MA_{1–4}^{-}$. Four pots filled with mixed CS and VA in a 1:1 (*v*/*v*) ratio, completing to 500 mL and 125 mL PS. Considering the CS only, 300–500 ppm $ZnSO_4$ were added. At least three sunflower seeds were sown in each pot.
- $B_{1–4}^{+}$. Four pots filled with 500 mL FCT and 125 mL PS. At least three sunflower seeds were sown and inoculated with a piece of 4-month old monoxenic culture (containing approximately 300 spores, mycelia and colonized roots).
- $B_{1–4}^{-}$. Four pots filled with 500 mL FCT and 125 mL PS. At least three sunflower seeds were planted in each pot.

On day 30, sunflower plantlets were thinned to one, leaving the most homogeneous with better leaves development in each pot. Plant cultures were maintained during 133 days in a room at controlled temperature (18–21 °C). As precautionary strategy, plants were irrigated only twice a week (50 mL per pot) in order to provide a sufficient amount of water for plant growth, and avoid the risk of any metals leaching.

2.3.3. Harvest and Sample Analyses

Representative soil samples (50 g) and plant biomass were taken from each pot on day 133. The soil samples were dried and micronized under 70 microns in size by vibrating rotary cup mill at 900 rpm motor speed and a standard 100 mL steel crew. The grinding containers incorporate an anvil ring and puck to pulverize the sample by an eccentric vibratory action. Physical and mineralogical characterization of soil samples were carried out by X-Ray Powder Diffraction (XRPD) as described in Guglietta et al. [1] and by Total Reflection X-Ray Fluorescence (TXRF). Sunflower plants were removed from each pot, and shoots and roots were separately harvested. Roots were carefully rinsed with distilled water, and then shoots and roots were dried in an oven (45 °C) to constant weight for registration of shoot and root dry weights, and subsequent quantification of chemical elements by the TXRF method (see: Section 2.3.4). To assess the mycorrhization level, subsamples of dried roots were stained with trypan blue solution following the modified technique of Phillips and Hayman [22]. The AM root colonization was checked according to Giovanneti and Mosse [23]. The frequency of mycorrhizal colonization was calculated as the percentage of root segments containing AM fungal structures. All measurements were taken under a Nikon Optiphot-2 light binocular microscope (Nikon Instruments Inc., Melville, LA, USA) at 100× magnification.

2.3.4. TXRF Analysis

The chemical determination of plant biomass and soil substrate from each pot was carried out by the TXRF method. For that, the entire plant sample was weighed and placed in a Teflon beaker with 3 mL sub-boiling HNO_3 and 1 mL H_2O_2, and then microwave digested. After digestion, the solution was transferred to a 10 mL volumetric flask (or 5 mL in case that the sample was smaller than 0.05 g) and made up to volume with milliQ water. A total of 10 µL of Ga 100 mg/L (Merck, Taufkirchen, Germany) was added as an internal standard to 1 mL of sample solution. Then, 5 µL of the solution was deposited on a quartz reflector and measured for 300 s in the TXRFS2 Picofox spectrometer (Bruker, Buenos Aires, Argentina) with Mo tube. For soils analysis, a 28 mm diameter pressed pellet was prepared with 3 g of dry sample. Elemental determination was carried out with a WDXRF S8 Tiger spectrometer (Bruker, Buenos Aires, Argentina), using the Quant Express application.

2.4. Bioextracting Potential (BP) in VDM

The estimation of BP of CRMs (Ba, Ga, P, Ti and Sr) and SRMs (Fe, Mn, Zn, Cr, As, Ni, Cu, Rb, Al, K, S, Ca) at TRL-6 by using the VDM containing contaminated soil was carried out considering the results achieved at TRL-2 experiment. The VDM is located at the Centro de Desarrollo Regional Los Reyunos of Universidad Tecnológica Nacional (San Rafael, Mendoza, Argentina) [8]. It consists of an external environment-isolated pool connected to collection chambers through a hydraulic system. The water runs through pipes connected to a reserve tank and a water pump that drives the vertical flow towards the pool, and the remaining fraction of percolated liquid is drained towards a collection chamber. The 15 cm-superficial layer, representing the growth substrate for the consortium *H.annuus-R. intraradices*, consisted of a homogeneous mixture of contaminated soil and volcanic ash (50:50; *v:v*) supplemented with 350 ppm of $ZnSO_4$ (Figure 5).

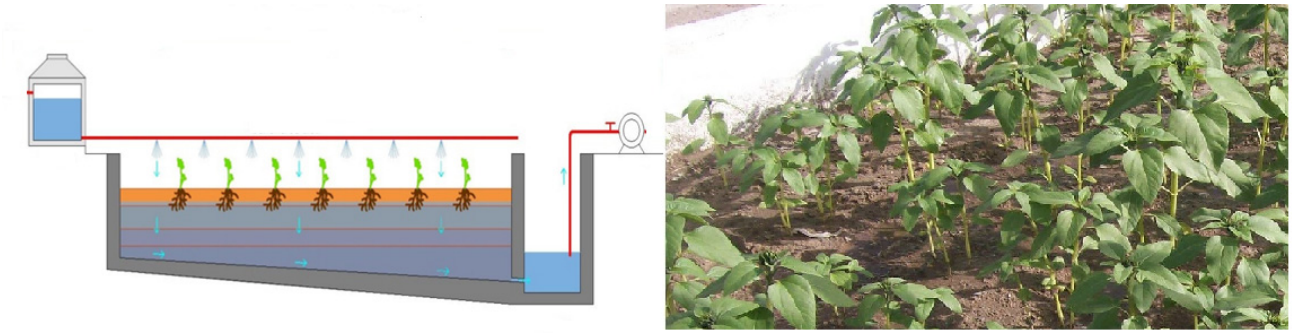

Figure 5. Diagram of the Vegetable Depuration Module (**left**) and the bioaugmentation system (**right**) (*Helianthus annuus—Rhizophagus intraradices)* with 2 m^3 volume of soil-ash (1:1) and 20 plants per m^2.

2.5. Calculations and Statistical Analyses

2.5.1. Bioconcentration Coefficients and Translocation Factor

The bioconcentration coefficient (BC) was calculated as the ratio between the concentration of the chemical element in plant tissue and soil (Equation (1)), for shoots and roots (BC_S and BC_R, respectively).

$$BC_{(S,R)} = C_{P(S,R)}/C_{soil} \quad (1)$$

where:

$C_{P(S,R)}$: concentration of element in the aerial (shoots, S) or radicular (roots, R) plant tissue (ppm)

C_{soil}: concentration of element in soil (ppm)

The translocation factor (TF) was calculated as the ratio between the concentration of the chemical element in shoots and roots (Equation (2)).

$$TF = C_{P(S)}/C_{P(R)} \quad (2)$$

where:

$C_{P(S)}$: concentration of element in the aerial plant tissue (shoots; ppm)

$C_{P(R)}$: concentration of element in the radicular plant tissue (roots; ppm)

BC and TF were calculated for the following SRMs (Fe, Mn, Zn, Cr, As, Ni, Cu, Rb, Al, K, S, Ca) and CRMs (Ba, Ga, P, Ti and Sr).

2.5.2. Bioextracting Potential (BP)

The estimation of BP of SRMs and CRMs by the VDM and the MAP system was calculated considering the concentration of each element in plant biomass obtained at TRL-2 experiment, and the total biomass grown in the VDM with 1 m^3 of contaminated soil, as follows (Equation (3))

$$BP\ (mg) = [(W_{tot(S)} \times C_{p(S)}) + (W_{tot(R)} \times C_{p(R)})]/1000 \quad (3)$$

where:

$W_{tot(S,R)}$: Total weight (g) of aerial (shoots, S) and radical (roots, R) plant tissue.
$C_{p(S,R)}$: concentration (ppm) of element in the aerial (shoots, S) or radicular (roots, R) plant tissue.

3. Results

MAP Test at TRL-2 Scale

During the experiment at TRL-2 scale, the sunflower plants grew healthy in all treatments. The AM fungus *Rhizophagus intraradices* strain GA5 colonized sunflower roots in both MA^+ and B^+ treatments after 133 days with typical AM fungal structures (vesicles, arbuscules and hyphae; Figure 6A), whilst no root colonization was found in the non-inoculated plants in control treatments (B^- and MA^-), as expected (Figure 6B). The MA^+ treatment showed the lowest value of AM root colonization with 5.0 ± 2.2% (mean ± standard error), and sunflower plants of the B^+ treatment reached 42.0 ± 2.71%. The AM inoculation with *R. intraradices* strain GA5 did not affect the total dry plant biomass in the contaminated treatment, while total biomass of mycorrhized sunflower plants grown in blank soil samples was significantly higher than contaminated soil (Table A1).

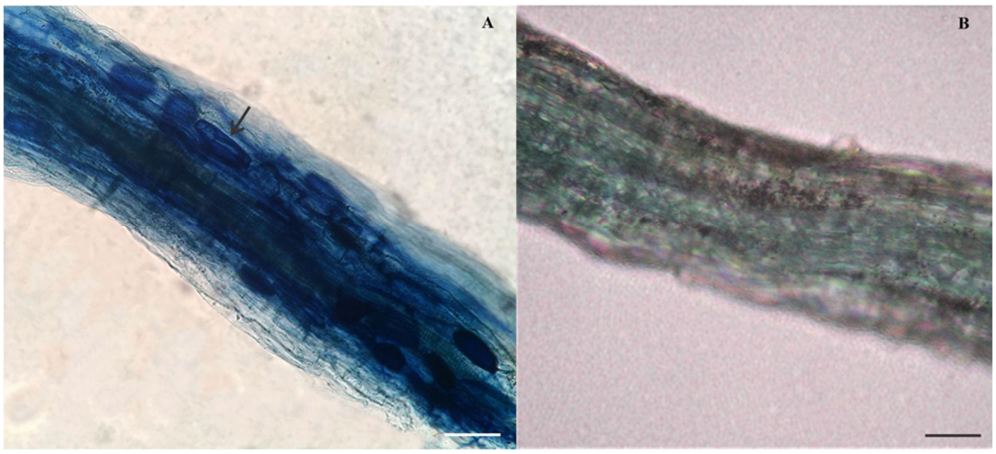

Figure 6. (**A**) Sunflower root fragment colonized by the AM fungus *Rhizophagus intraradices* (strain GA5) after 133 days (MA_1^+ treatment). Detail of the vesicles of AM fungus (black arrow); (**B**) uncolonized root of sunflower plant in control treatment (MA_1^- treatment); Bars: 200 μm.

The average concentrations of SRMs (Fe, Mn, Zn, Cr, As, Ni, Cu, Rb, Al, K, S and Ca) and CRMs (Ba, Ga, P, Ti and Sr) in soil samples taken from each pot of the contaminated and blank treatments, as well as in sunflower plant biomass after 133 days of growth are reported in Tables 1 and 2. The $BC_{(S,R)}$ and TF values of these elements for all treatments are summarized in Table 3.

Table 1. Mean concentration of CRMs in samples from pots containing contaminated soil (MA) and blank soil (B), as well as in biomass ($C_{p(S,R)}$), with and without mycorrhization (+, −). Standard error (SE) is reported in brackets.

Sample Type	Sample ID	N	Ga (ppm)	P (ppm)	Ti (ppm)	Sr (ppm)	Ba (ppm)
Contaminated	MA^-	4	12.88 (0.572)	731 (32.8)	2575 (94.65)	110 (3.47)	2550 (86.6)
	MA^+	4	20.13 (1.994)	711 (15.14)	2675 (25)	112(4.94)	2600 (40.8)

	$C_{P(S)^+}$	2	31.50 (9.596)	3803 (209.1)	9,5 (0.5)	410 (172)	7.85 (0.15)
	$C_{P(S)^-}$	2	13.70 (1.616)	2878 (158.6)	16 (1)	254 (9.60)	11.5 (0.5)
	$C_{P(R)^+}$	2	25.55 (3.889)	1228 (35.86)	446 (24.24)	79(4.04)	98.5 (1.51)
	$C_{P(R)^-}$	2	22.00 (1.010)	880 (27.27)	947.5 (53)	138 (7.07)	163.5 (6.5)
Blank	B^+	4	5.00 (0.34)	2125 (25.00)	1275 (25)	1100 (57.7)	431.25 (21.29)
	$C_{P(S)^+}$	2	3.02 (0.75)	3583 (200.1)	9 (3)	229 (1.01)	8.0 (1.0)
	$C_{P(R)^+}$	2	3.00 (0.10)	1412 (39.39)	509 (11.11)	106 (5.56)	28.5 (1.51)

Table 2. Mean concentration of SRMs in samples from pots containing contaminated soil (MA) and blank soil (B), as well as in biomass ($C_{P(S,R)}$), with and without mycorrhization (+, −). Standard error (SE) is reported in brackets.

Sample Type	Sample ID	N	Mn (%)	Fe (%)	As (ppm)	Zn (ppm)	Cr (ppm)	Ni (ppm)	Cu (ppm)	Rb (ppm)	Al (ppm)	K (%)	S (ppm)	Ca (%)
Contaminated	MA^-	4	4.93 (0.13)	11.2 (0.26)	12.5 (0.59)	1500 (108)	110 (7.67)	67.0 (2.24)	60.3 (1.65)	78.3 (1.49)	62,500 (1040.8)	2.30 (0.04)	1195 (113.1	1.12 (0.10)
	MA^+	4	5.55 (0.03)	12.2 (0.06)	23.2 (1.24)	1475 (25.0)	113.3 (2.93)	72.3 (1.49)	64.5 (2.53)	80.5 (1.76)	64,750 (250)	2.20 (0.04)	1125 (125)	1.05 (0.04)
	$C_{P(S)^+}$	2	0.052 (0.003)	0.03 (0.001)	4.05 (0.05)	1328 (37.9)	2.80 (0.20)	1.80 (0.10)	16.5 (0.51)	116 (4.04)	0.95 (0.05)	7.70 (0.40)	5945 (162.1)	2.25 (0.15)
	$C_{P(S)^-}$	2	0.05 (0.003)	0.03 (0.002)	1.50 (0.10)	1410 (39.4)	0.65 (0.05)	1.00 (0.10)	14.0 (1.01)	102 (2.53)	0.93 (0.07)	7.10 (0.20)	6189 (162.1)	2.06 (0.06)
	$C_{P(R)^+}$	2	0.455 (0.024)	1.19 (0.06)	6.50 (0.505)	1162 (32.3)	29.5 (1.52)	38.0 (2.02)	17.5 (0.51)	12.5 (0.51)	5550 (2272.4)	4.65 (0.15)	16,885 (672.3)	0.99 (0.02)
	$C_{P(R)^-}$	2	0.74 (0.04)	2.13 (0.13)	6.50 (0.505)	1717 (92.4)	10.00 (1.01)	14.0 (10.0)	36.0 (2.02)	109 (3.54)	21,375 (419.2)	5.20 (0.15)	13,772 (307.6)	2.46 (0.08)
Blank	B^+	4	0.06 (0.001)	1.43 (0.03)	8.78 (0.41)	210.8 (9.4)	86.50 (9.1)	42.3 (0.75)	108 (2.68)	212 (14.1)	13,625 (239.3)	1.33 (0.05)	3525 (110.9)	5.33 (0.06)
	$C_{P(S)^+}$	2	0.007 (0.0006)	0.01 (0.001)	1.65 (0.25)	54.50 (4.6)	3.45 (1.26)	2.80 (1.31)	15.0 (0.00)	76.0 (1.01)	8.9 (0.04)	5.40 (0.10)	2045 (49.5)	1.86 (0.11)
	$C_{P(R)^+}$	2	0.03 (0.002)	0.22 (0.01)	3.55 (0.02)	166.5 (4.6)	12.0 (1.01)	6.45 (0.25)	42.5 (2.53)	33.0 (2.02)	13,900 (303,04)	1.06 (0.03)	1725 (29.3)	4.32 (0.09)

Table 3. Average bioconcentration coefficient (BC) in shoots (S) and in roots (R) of plants grown on mycorrhized (+) and not mycorrhized (−) systems. Standard error (SE) is reported in brackets.

Sample ID	Parameter	Mn	Ga	Fe	P	As	Zn	Ti	Sr	Cr	Ni	Cu	Rb	Al	Ba	K	S	Ca
MA^+	$BC_S{}^+$	0.009 (0.001)	1.565 (0.632)	0.002 (0.0001)	5.349 (0.408)	0.175 (0.012)	0.900 (0.046)	0.004 (0.0002)	3.653 (3.356)	0.025 (0.002)	0.025 (0.002)	0.256 (0.018)	1.441 (0.082)	0.000 (0.000)	0.003 (0.0001)	3.500 (0.247)	5.284 (0.731)	2.138 (0.233)
	$BC_R{}^+$	0.082 (0.005)	1.270 (0.319)	0.098 (0.006)	1.726 (0.087)	0.281 (0.162)	0.788 (0.035)	0.167 (0.011)	0.704 (0.388)	0.261 (0.020)	0.526 (0.039)	0.271 (0.019)	0.155 (0.010)	0.086 (0.035)	0.038 (0.001)	2.114 (0.107)	15.008 (2.265)	0.936 (0.053)
	TF^+	0.114 (0.013)	1.233 (0.808)	0.023 (0.003)	3.098 (0.393)	0.623 (0.401)	1.142 (0.064)	0.021 (0.002)	5.190 (3.973)	0.095 (0.012)	0.047 (0.005)	0.943 (0.056)	9.280 (0.698)	0.0002 0.0001	0.080 (0.003)	1.656 (0.141)	0.352 (0.024)	2.284 (0.189)
MA^-	$BC_S{}^-$	0.011 (0.001)	1.064 (0.173)	0.003 (0.0002)	3.937 (0.394)	0.125 (0.014)	0.940 (0.100)	0.006 (0.001)	2.310 (0.161)	0.006 (0.001)	0.015 (0.002)	0.232 (0.023)	1.297 (0.057)	0.000 (0.000)	0.005 (0.0004)	3.087 (0.143)	5.181 (0.626)	1.835 (0.224)
	$BC_R{}^-$	0.150 (0.012)	1.709 (0.154)	0.190 (0.016)	1.204 (0.091)	0.522 (0.065)	1.144 (0.144)	0.368 (0.034)	1.257 (0.104)	0.091 (0.016)	0.209 (0.022)	0.598 (0.050)	1.387 (0.072)	0.342 (0.012)	0.064 (0.048)	2.283 (0.106)	11.529 (1.349)	2.187 (0.270)
	TF^-	0.073 (0.008)	0.623 (0.157)	0.014 (0.002)	3.271 (0.576)	0.231 (0.034)	0.821 (0.067)	0.017 (0.002)	1.837 (0.164)	0.065 (0.012)	0.071 (0.012)	0.389 (0.050)	0.936 (0.054)	0.000 (0.000)	0.070 (0.006)	1.352 (0.078)	0.449 (0.022)	0.839 (0.051)

There was a marked difference for $BC_{(S,R)}$ and TF in the elements under study when blank and contaminated soil were compared. The $BC_{(S,R)}$ and TF values when sunflower plants were colonized followed the order: P = 5.34 > S > Sr > K > Ca > Ga > Rb > Zn > Cu > As > Ni = Cr > Mn > Ti > Ba > Fe > Al = 0.00 for $BC_{(S)}$, while for $BC_{(R)}$ was: S = 15.00 > K > P> Ga > Ca > Zn > Sr > Ni > As > Cu > Cr > Ti > Rb > Fe > Al > Mn > Ba and for TF was: Rb = 9.28 > Sr > P > Ca > K > Ga > Zn > Cu > As > S > Mn > Cr > Ba > Ni > Ti = Fe > Al. Significant differences in BC and TF values for all the elements, except for Ga, were observed between soil contaminated with or without AM inoculation for at least one of the parameters studied (Table 4). No differences in the metal concentrations in blank soil were observed in presence or absence of the AM fungus (Table A2). The effect of AM colonization on TF values was different for the elements under study. Mn, Fe, Zn, Cr, As, Cu, Rb, Al, Ba, K, Ca, Sr and Ti were affected by increasing their TF; no significant effects for TF were detected for Ga and P, while S and Ni decreased it, as summarized in Table 4. In contrast, the AM colonization increased the $BC_{(S)}$ for P, As, Cr, Ni, Rb, K and decreased for Mn, Fe, Ti and Ba. Beside the $BC_{(R)}$ for P, Cr, S and Ni increased, but for Mn, Fe, As, Zn, Ti, Cu, Rb, Sr, Al, Ba and Ca a decrease was observed (Table 4).

Table 4. Overall effect of arbuscular mycorrhizal colonization on $BC_{(S)}$, $BC_{(R)}$ and TF, compared to control tests (not mycorrhized) (+, increase; −, decrease; =, no significant effect).

Parameter	Mn	Ga	Fe	P	As	Zn	Ti	Cr	Ni	Cu	Rb	Sr	Al	Ba	K	S	Ca
BC_S	(−)	(=)	(−)	(+)	(+)	(=)	(−)	(+)	(+)	(=)	(+)	(=)	(=)	(−)	(+)	(=)	(=)
BC_R	(−)	(=)	(−)	(+)	(−)	(−)	(−)	(+)	(+)	(−)	(−)	(−)	(−)	(−)	(=)	(+)	(−)
TF	(+)	(=)	(+)	(=)	(+)	(+)	(+)	(+)	(−)	(+)	(+)	(+)	(+)	(+)	(+)	(−)	(+)

The extractive power of MAP in VDM is shown in Table 5 considering 290 plants and 1 m^3 of contaminated soil.

Table 5. Estimated elements extracting potential by MAP in a VDM containing 1 m^3 of contaminated soil. Standard Deviation is reported in brackets.

Parameter	Mn (ppm)	Fe (ppm)	Ga (ppm)	P (ppm)	As (ppm)	Zn (ppm)	Ti (ppm)	Cr (ppm)	Ni (ppm)	Cu (ppm)	Rb (ppm)	Sr (ppm)	Al (ppm)	Ba (ppm)	K (ppm)	S (ppm)	Ca (ppm)
$C_{P(S)^+}$	520 (42)	270,5 (20,5)	31.5 (13,4)	3803 (292)	4.05 (0.07)	1328 (53)	9.5 (0.7)	2.8 (0.3)	1.8 (0.1)	16.5 (0.7)	116 (5.66)	410 (240)	0.95 (0.07)	7.85 (0.21)	77,000 (5657)	5944.5 (227)	22,500 (2121)
$C_{P(R)^+}$	4550 (343)	11,888 (898)	25.5 (5,4)	1228 (50)	6.5 (0.7)	1162 (45)	446 (34)	29.5 (2.1)	38 (2.8)	17.5 (0.71)	12.5 (0.71)	79 (5.7)	5550 (3181)	98.5 (2.12)	46,500 (2121)	16,885 (941)	9850 (212)
Extracting g/VDM *	34.82	60.01	1.017	114.7	0.145	43.22	2.199	0.208	0.216	0.550	3.392	12.14	23.99	0.6515	2417	243.9	690.0

* VDM contained 1 m^3 of contaminated soil, the calculation can be also expressed as per cubic meter of contaminated soil.

4. Discussion

The MAP system at TRL-2 showed good extraction capabilities for many SRMs and CRMs in terms of BC and TF, although biomass growth observed in mining waste substrate was relatively low. Likewise, different behaviors of accumulation and translocation for each chemical element were observed in the MAP system. On the other hand, the mycorrhized soil at the end of the experiment had a significant higher concentration for Ga, Mn, Fe, As, Ni, Cu, Al than the soil without mycorrhization, while for the rest of the elements there were no significant differences (P, Ti, Sr, Zn, Cr, Rb, Ba, K, S and Ca). This could be due to the accumulation of elements in fungal structures such as mycelium and/or spores [24,25].

In regard to Ca, Zn and Cu, no differences were found in the $BC_{(S)}$ between mycorrhized and non-mycorrhized plants. However, the TF values were high in mycorrhized plants for these elements. It is known that Cu ions are involved in photosynthesis, respiration, diverse enzymes of antioxidative defense and hormone metabolism [26]. In a previous work, we found that the same MAP system was highly efficient in bioextracting Cu than other metals when the mass balance was analyzed in VDM [8]. We disclaimed that alkaline substrate could facilitate the mobility of this metal and increase the total Cu fraction available for plants. In opposition, the BP value of Cu by the MAP in the VDM containing Fe and Mn mining wastes was not notorious (Table 5). Likewise, the colonized roots of sunflower plants did not accumulate Ca, Zn and Cu but non-colonized roots did. Cornejo et al. [24] demonstrated that AM fungi usually store Cu in vesicles and spores in roots for minimizing the toxic effects on plant and fungal metabolism. Probably, no Cu accumulation in root tissues was observed because of the low intensity of AM colonization by *R. intraradices* strain GA5 after 133 days. In addition, in contrast with our previous results [8], Zn was not accumulated in mycorrhized plant roots. These discrepancies could be due to the characteristics/properties of the multi-metal mining substrate under study. The different concentrations of each metal could lead to competition for specific sites of entry into the plant and the AM fungal structures. It was reported that the extraradical mycelium and glomalin released in soil by AM fungi are capable of sequestering Ca, Zn and Cu ions limiting their entrance to the roots [25,27]. In addition, Chen et al. [28] observed a higher affinity of Cu and Zn ions in the fungal biomass rather than roots or shoots of the host plants. Otherwise, the storage of Ca ions in external hyphae might be enhancing the nutrient absorption, as we observed the higher P concentrations in shoots and roots of mycorrhized sunflower plants. The acidification of the hyphosphere (the zone of soil adjacent to hyphae) caused by the regulation of transmembrane fluxes potentially promotes the absorption of nutrients between hyphae and the soil environment under stress conditions [29]. As in Scotti et al. [8] the BP of Zn by the MAP system in the MDV reached a very good performance, reaching a value of 43.2 g/m^3, even improving the previously found value of 29.3 g/m^3. In the same way, the BP for Ca was very important (690 g/m^3).

The concentration of S was higher in roots and the TF value was lower in mycorrhized plants than non-mycorrhized; no differences in $BC_{(S)}$ between treatments were found. Allen and Shachar-Hill [30] demonstrated that AM fungi are capable of increasing root S contents by 25% in a moderate (not growth-limiting) concentration of sulfate. Additionally, Aziz et al. [31] showed that sulfur supplementation up to 80 ppm in soil increases the content of K and Ca in plant tissues, and enhances the photosynthetic rate, water content and tolerance to salinity in *H. annuus* without limiting effect; although higher sulfur concentrations were present in contaminated soils used in our study, the concomitant increase of Ca and K was observed.

Mn and Ti are essential micronutrients involved in the activation of Krebs cycle enzymes and the chlorophyll synthesis [32,33]. Additionally, Ti is considered a CRM in the fourth list of the European Commission (COM 2020/474, EC) [34]. In our work, Mn and Ti were translocated more efficiently to aerial parts when the AM fungus *R. intraradices* was present. However, non-mycorrhized plants accumulated more Mn and Ti in roots and shoots. The uptake of Mn was repeatedly found to be lower in mycorrhized plants [35]. The negative effect on Mn uptake was attributed to a shift in the composition and activity of rhizosphere microorganisms caused by inoculation with AM fungi, which decreases the abundance of Mn reducers microbes [36]. However, the BP potential of Mn for the MAP system in VDM was effective, as in Scotti et al. [8] but mainly due to percolation and recovery in the collecting chamber of the VDM. Probably, the high concentration of Mn of the mining wastes translates it into significant amounts of Mn recovering into biomass (34.82 g/m^3). Our study showed that AM colonization augmented Cr and Ni uptake in shoots and roots of sunflowers, but also contributed to enhance nutrient acquisition by high P contents in plants. It is widely known that AM fungi improve nutritional status of

colonized plants, mainly by P and N uptake [9] and contribute to the enhancement of Ni and Cr in sunflower biomass [4]. This result is of great importance given that P is a valuable CRM and an essential nutrient for plant growth. As in Scotti et al. [8], there was not a good recovery in biomass of either Cr or Ni (0.21 g/m^3), but the recovery of P was very important (114.7 g/m^3).

According to bioaccumulation results, mycorrhized plants accumulated more As, Sr and Rb in shoots than in roots, and showed higher TF values than non-mycorrhized plants. Besides, the behavior of K ions was like these elements, but no differences were found in K concentrations in roots of mycorrhized and non-mycorrhized plants. K is one of the most abundant chemical elements in soil composition, but it very low availability limits plant growth. Previously, it was observed that AM symbiosis increased K acquisition in Asteraceae plants [37]. Interestingly, a strong correlation between K and P during AM symbiosis was reported [38], coinciding with our results. Otherwise, Rb is an analog for K, which is taken up along the same pathways as K and typically occurs at very low levels in soils and plant tissues [39]. We also observed the competitive behavior between K and Rb for the potential recovery in the VDM. In a previous work [40], it was found that As is predominantly deposited into leaves of sunflowers when grown in arsenic contaminated soil. The chemical similarity of P and As, combined with the mycorrhizal role in P nutrition, provides the likelihood that AM fungi may enhance As uptake [41]. Given that AM symbiosis enhanced P uptake in sunflower plants, it was possible that the AM fungus also increased the uptake of As in shoot tissues. In accordance with our previous work [8], Sr (CRM) showed high translocation to shoots and accumulation within above ground tissues. Many authors have confirmed that Sr can be accumulated in leaves, leaf trichomes and stems of several plant species [42,43]. The accumulation of toxic elements in trichomes was widely cited as a tolerance mechanism of plants subjected to stressful toxic conditions [43]. The Sr bioextracting potential was moderate (12.14 g/m^3), as was also demonstrated in Scotti et al. [8].

No differences in BC and TF values for Fe were found between mycorrhized and non-mycorrhized plants. Ferrol et al. [36] noticed that the effect of mycorrhizal colonization on Fe concentration in plant tissues is variable and inconsistent. The external mycelium and glomalin in soil immobilize Fe ions as it was demonstrated by detection of abundant crystal-like aggregates present on the mucilaginous outer hyphal wall layers of AM fungi [27]. It was demonstrated that Fe elements accumulated at the hyphosphere enhance the nutrient absorption by hyphae, as Ca ions performance [29]. In opposition, the biomass extraction in the VDM for Fe was important due to the high concentration of the metal in the mining wastes.

The Ga accumulation in shoots and roots did not differ between mycorrhized and non-mycorrhized plants. Jensen et al. [44] demonstrated that movement of Ga into the aboveground portions of perennial ryegrass (*Lolium perenne* L.) was low ($BC_{(S)}$: 0.0037), concluding that the mobility of Ga in the soil-plant system is low compared to other common trace element contaminants. While Yu et al. [45] demonstrated roots of rice seedlings were the dominant site for Ga accumulation and the total Ga accumulation rates were positively correlated to its concentrations. In our work, we agree with these researchers on the increase in Ga content in the roots when there is no mycorrhization (22 ppm in roots vs. 13.7 ppm in shoots), while when there is mycorrhization no significant differences were detected. The bio-extraction in the VDM reached an interesting value, thus increasing the commercial importance of Ga as CRM by using this biotechnology. It is known that Ga is chemically similar to Al. Others reports have indicated that AM fungi increased or did not affect Al accumulation in leaves and roots of host plants, and that glomalin and fungal hyphae modulate interactions between plants and soil Al [46]. Accordingly, Al followed the same behavior that Ga ions after observing an increase in roots when there is no AM colonization. More studies should be performed to analyze the role of AM fungal mycelium in Ga sequestration.

Finally, Ba did not show high BP (0.65 g/m^3), as previously reported by Coscione et al. [47]. In the same way, Ba control concentration in shoots was coincident with these authors. To the author's knowledge, no studies were found about Ba accumulation in sunflower plants colonized by AM fungi.

The average estimated BP encourages the subsequent recovery of SRMs and CRMs by hydrometallurgical techniques, with final purification by selective electrodeposition, as a viable and cost-effective option. For a sustainable recovery of metals from an economic and environmental point of view, the application of hydrometallurgical processes is important, because they allow, through the use of specific innovative reagents and the application of electrochemical techniques, their selective recovery at high degree of purity, which determines an appropriate commercial reuse. The fast kinetics guarantees the economy of the process because it allows reduction of the capital costs (smaller capacity reactors can be used) and the energy requirement, the latter representing an advantage also from the environmental point of view.

Assuming an integrated process circuit consisting of a leaching phase of accumulated and concentrated SRMs and CRMs, and subsequent purification by electrochemical methods, with purity levels of more than 90% will allow an industrial reuse of SRMs and CRMs, in the context of a circular economy approach [48].

5. Conclusions

In summary, the present work confirmed that it is possible to apply the MAP system in contaminated soils from mining areas classified by remote sensing as Class 2 and 4, and to carry out the bio-extraction of all the elements studied. Only S, Ni, P and Ga did not show an increase in the TF under the conditions of the experiment, the other elements under study showed a significant increase in the TF when plants were mycorrhized. Despite such promising results, it must be noticed that process conditions must be optimized to maximize plant growth and sustain a significant recovery of SRMs and CRMs by hydrometallurgical methods. It is important to monitor pH and Eh (BS ISO 11271:2002) values at various depths of soil, in order to relate the solubilization of the elements with their bioaccumulation. In addition, the simulation of MAP at TRL-6 (i.e., in a VDM) yielded novel and interesting results: the quantity of biomass extracted in the VDM is a more reliable indicator of the bio-extraction potential than the analysis of the bioaccumulation coefficient, which is directly depending on the metal concentration in soil and the possible inhibition of enzymes in metabolic pathways. Results are encouraging and the application of such multidisciplinary approach can be important to develop a circular model for sustainable exploitation of mining residues.

Author Contributions: Conceptualization, A.S., V.S. and S.M.; methodology, A.S., V.S., G.C. and D.G.; software, D.G.; validation, A.S., V.S. and A.G.; formal analysis, F.T., E.T. and D.P.; investigation, A.S. and V.S.; resources, A.S., A.G. and S.U.; data curation, A.S. and V.S.; writing—original draft preparation, A.S., V.S., S.M. and D.G.; writing—review and editing, S.M., A.G. and S.U.; visualization, A.G. and S.U.; supervision, A.S., S.M. and G.C.; project administration, A.S., S.M. and S.U.; funding acquisition, A.S., M.G. and S.U. All authors have read and agreed to the published version of the manuscript.

Funding: This research was funded by TECO Project e Technological eco-innovation for the quality control and the decontamination of polluted waters and soils-reference: "EuropeAid/135-474/DD/ACT/IN, "EU-India Research and Innovation Partnership"—and by S&T Cooperation Programme between Italian Republic and Argentina, financially supported by Italian Ministry of Foreign Affairs and International Cooperation (MAECI) and Ministry of Science, Technology and Innovation of the Argentine Republic (SGCTeIP), entitled: "Integrated multidisciplinary approach for the identification and recovery of raw materials from mining waste, by remote sensing".

Institutional Review Board Statement: Not applicable.

Informed Consent Statement: Not applicable.

Data Availability Statement: The study did not report any data.

Acknowledgments: We acknowledge to Jorge Álvarez, Paola Babay, Florencia Gonzalez, and Roxana Leguizamón from Chemistry Management, FRX Laboratory of National Atomic Energy Commission, Buenos Aires, Argentina for their technical assistance in FRX fluorescence analyses.

Conflicts of Interest: The authors declare no conflict of interest.

Appendix A

Table A1. Concentrations of elements in mycorrhized and non-mycorrhized plants grown in blank soil. Standard Deviation is reported in brackets.

Treatment	N	Mn (%)	P (ppm)	As (ppm)	Ga (ppm)	Zn (ppm)	Ti (%)	Cr (ppm)	Ni (ppm)	Cu (ppm)	Rb (ppm)	Fe (%)	Sr (ppm)	Al (%)	Ba (%)	K (%)	S (ppm)	Ca (%)
B^-	4	0.068 (0.011)	2275 (170.8)	7.050 (2.106)	5.125 (0.378)	213.8 (7.411)	0.135 (0.006)	87.25 (10.72)	43.50 (3.317)	110.5 (3.697)	206.8 (48.03)	1.475 (0.096)	1081 (114.3)	1.525 (0.250)	0.043 (0.006)	1.350 (0.100)	3450 (264.6)	5.500 (0.316)
B^+	4	0.062 (0.002)	2125 (50.00)	8.775 (0.818)	5.000 (0.683)	210.8 (18.79)	0.128 (0.005)	86.50 (18.23)	42.25 (1.500)	108.0 (5.354)	211.5 (28.21)	1.425 (0.050)	1100 (115.5)	1.363 (0.048)	0.043 (0.004)	1.325 (0.096)	3525 (221.7)	5.325 (0.126)

Table A2. Biomass per specimen (sp) of *Helliantus annuus* grown in contaminated and blank soil. Standard Deviation is reported in brackets.

Sample Type	Biomass (g/sp)	M^+	M^-
Contaminated	Shoots	0.24 ^{a} (0.03)	0.24 ^{a} (0.02)
	Roots	0.02 ^{b} (0.01)	0.02 ^{b} (0.004)
Blank	Shoots	0.35 ^{c} (0.01)	0.23 ^{a} (0.02)
	Roots	0.11 ^{d} (0.001)	0.02 ^{b} (0.002)

$^{a–d}$: different letters correspond to significant differences.

References

1. Guglietta, D.; Belardi, G.; Cappai, G.; Casentini, B.; Godeas, A.; Milia, S.; Passeri, D.; Salvatori, R.; Scotti, A.; Silvani, V.; et al. Toward a multidisciplinary strategy for the classification and reuse of iron and manganese mining wastes. *Chem. J. Mold.* **2020**, *15*, 21–30.
2. Mathieux, F.; Ardente, F.; Bobba, S.; Nuss, P.; Blengini, G.; Alves Dias, P.; Blagoeva, D.; Torres De Matos, C.; Wittmer, D.; Pavel, C.; et al. *Critical Raw Materials and the Circular Economy–Background Report*; Publications Office of the European Union: Bruxelles, Belgium, 2017, doi:10.2760/378123 JRC108710.
3. Glick, B.R. Phytoremediation: Synergistic use of plants and bacteria to clean up the environment. *Biotechnol. Adv.* **2003**, *21*, 383–393.
4. Ker, K.; Charest, C. Nickel remediation by AM colonized sunflower. *Mycorrhiza* **2010**, *20*, 399–406.
5. Kastori, P.; Petrovic, N.; Petrovic, M. Effects of lead on water relations, proline concentration and nitrate reductase activity in sunflower plants. *Acta Agron. Hungar.* **1996**, *44*, 21–28.
6. Turgut, C.; Pepe, M.K.; Cutright, T.J. The effect of EDTA and citric acid on phytoremediation of Cd, Cr, and Ni from soil using Helianthus annuus. *Environ. Pollut.* **2004**, *131*, 147–154.
7. Davies, F.T.; Puryear, J.D.; Newton, R.J.; Egilla, J.N.; Saraiva Grossi, J.A. Mycorrhizal fungi increase chromium uptake by sunflower plants: Influence on tissue mineral concentration, growth, and gas exchange. *J. Plant. Nutr.* **2002**, *25*, 2389–2407.
8. Scotti, A.; Silvani, V.; Cerioni, J.; Visciglia, M.; Benavidez, M.; Godeas, A.A. Pilot testing of a bioremediation system of water and soils contaminated with heavy metals: Vegetable Depuration Module. *Int. J. Phytoremediation* **2019**, *21*, 899–907.
9. Smith, S.E.; Read, D.J. *Mycorrhizal Symbiosis*, 3rd ed.; Academic Press: New York, NY, USA, 2008.
10. Lenoir, I.; Fontaine, J.; Lounès-Hadj Sahraoui, A. Arbuscular mycorrhizal fungal responses to abiotic stresses: A review. *Phytochemistry* **2016**, *123*, 4–15.
11. Gohre, V.; Paszkowski, U. Contribution of the arbuscular mycorrhizal symbiosis to heavy metal phytoremediation. *Planta* **2006**, *223*, 1115–1122.
12. Yang, Y.; Liang, Y.; Han, X.; Chiu, T.Y.; Ghosh, A.; Chen, H.; Tang, M. The roles of arbuscular mycorrhizal fungi (AMF) in phytoremediation and tree-herb interactions in Pb contaminated soil. *Sci. Rep.* **2016**, *6*, 20469.
13. Rivelli, A.R.; De Maria, S.; Puschenreiter, M.; Gherbin, P. Accumulation of cadmium, zinc, and copper by *Helianthus annuus* L.: Impact on plant growth and uptake of nutritional elements. *Int. J. Phytoremediation* **2012**, *14*, 320–334.
14. Scotti, A.; Godeas, A.; Silvani, V. Sistema Biorremediador Para Tratamiento de Suelo y/o Aguas Contaminadas. Argentina Patent 130100620, 22 October 2014.

15. Scotti, A.; Milia, S.; Silvani, V.; Cappai, G.; Guglietta, D.; Trapasso, F.; Belardi, G.; Salvatori, R.; Tempesta, E.; Passeri, D.; et al. Development of an integrated multidisciplinary strategy for gallium, iron and manganese recovery from mining residues in a context of circular economy. In Proceedings of the International Center of Earth Sciences Conference, Mendoza, Argentina, 23 November 2020; Martín, G., Dino, F., Eds.; CNEA: Buenos Aires City, Argentina, 2021; pp. 898–910.
16. Kadlec, R.H.; Knight, R.L.; Vymazal, J.; Brix, H.; Cooper, P. *Constructed Wetlands for Pollution Control*; IWA Publishing: London, UK, 2000.
17. Mena, J.; Rodríguez, L.; Núñez, J.; Fernández, F.J.; Villaseñor, J. Design of horizontal and vertical subsurface flow constructed wetlands treating industrial wastewaters. *WIT Trans. Ecol. Environ.* **2008**, *111*, 555–564.
18. Madera-Parra, C.A. Treatment of landfill leachate by polyculture constructed wetlands planted with native plants. *Ing. Comptet.* **2016**, *18*, 183–192.
19. Ibañez, J. Niveles de madurez de la tecnología [Technology readiness levels: TRLS]: Una introducción. *Econ. Indus.* **2014**, *393*, 165–171.
20. Silvani, V.A.; Fernández Bidondo, L.; Bompadre, M.J.; Pérgola, M.; Bompadre, A.; Fracchia, S.; Godeas, A.M. Growth dynamics of geographically different arbuscular mycorrhizal fungal isolates belonging to the '*Rhizophagus* clade' under monoxenic conditions. *Mycologia* **2014**, *106*, 963–975.
21. Bompadre, M.J.; Silvani, V.A.; Fernández Bidondo, L.; Ríos de Molina, M.C.; Colombo, R.; Pardo, A.G.; Godeas, A. Arbuscular mycorrhizal fungi alleviate oxidative stress in pomegranate plants growing under different irrigation conditions. *Botany* **2014**, *92*, 187–193.
22. Phillips, J.M.; Hayman, D.S. Improved procedures for clearing roots and staining parasitic and vesicular-arbuscular mycorrhizal fungi for rapid assessment of infection. *Trans. Br. Mycol. Soc.* **1970**, *55*, 158–160.
23. Giovannetti, M.; Mosse, M. An evaluation of techniques for measuring vesicular arbuscular infection in roots. *New Phytol.* **1980**, *84*, 589–600.
24. Cornejo, P.; Pérez-Tienda, J.; Meier, S.; Valderas, A.; Borie, F.; Azcón-Aguilar, C.; Ferrol, N. Copper compartmentalization in spores as a survival strategy of arbuscular mycorrhizal fungi in Cu-polluted environments. *Soil Biol. Biochem.* **2013**, *57*, 925–928.
25. Gonzalez-Chavez, C.; D'Haen, J.; Vangronsveld, J.; Dodd, J.C. Copper sorption and accumulation by the extraradical mycelium of different *Glomus* spp. (arbuscular mycorrhizal fungi) isolated from the same polluted soil. *Plant Soil* **2020**, *240*, 287–297.
26. Yruela, I. Copper in plants. *Braz. J. Plant Physiol.* **2005**, *17*, 145–156.
27. Gonzalez-Chavez, M.; Carrillo-Gonzalez, R.; Wright, S.F.; Nichols, K.A. The role of glomalin, a protein produced by arbuscular mycorrhizal fungi, in sequestering potentially toxic elements. *Environ. Pollut.* **2004**, *130*, 317–323.
28. Chen, B.; Christie, P.; Li, X. A modified glass bead compartment cultivation system for studies on nutrient and trace metal uptake by arbuscular mycorrhiza. *Chemosphere* **2001**, *42*, 185–192.
29. Xu, L.J.; Hao, Z.P.; Xie, W.; Li, F.; Chen, B.D. Transmembrane H + and Ca 2+ fluxes through extraradical hyphae of arbuscular mycorrhizal fungi in response to drought stress. *Chin. J. Plant. Ecol.* **2018**, *42*, 764–773.
30. Allen, J.W.; Shachar-Hill, Y. Sulfur Transfer through an Arbuscular Mycorrhiza. *Plant. Physiol.* **2009**, *149*, 549–560.
31. Aziz, A.; Muhammad, A.; Sultan, S.; Muhammad, A.; Naeem, A.; Sher, M.S.; Allah, W.; Ali, R.; Babar, H.B. Optimizing sulfur for improving salt tolerance of sunflower (*Helianthus annuus* L.). *Soil Environ.* **2019**, *38*, 222–233.
32. Ducic, T.; Polle, A. Transport and detoxification of manganese and copper in plants. *Braz. J. Plant. Physiol.* **2005**, *17*, 103–112.
33. Lyu, S.; Wei, X.; Chen, J.; Wang, C.; Wang, X.; Pan, D. Titanium as a Beneficial Element for Crop Production. *Front. Plant. Sci.* **2017**, *8*, 597.
34. European Commission, COM 2020/474 Final. Available online: https://eur-lex.europa.eu/legal-content/EN/TXT/?uri=CELEX:52020DC0474 (accessed on 21 July 2021).
35. Correa, A.; Cruz, C.; Pérez-Tienda, J.; Ferrol, N. Shedding light onto nutrient responses of arbuscular mycorrhizal plants: Nutrient interactions may lead to unpredicted outcomes of the symbiosis. *Plant. Sci.* **2014**, *221–222*, 29–41.
36. Ferrol, N.; Tamayo, E.; Vargas, P. The heavy metal paradox in arbuscular mycorrhizas: From mechanisms to biotechnological applications. *J. Experim. Bot.* **2016**, *67*, 6253–6265.
37. Garcia, K.; Zimmermann, S.D. The role of mycorrhizal associations in plant potassium nutrition. *Front. Plant Sci.* **2014**, *5*, 337.
38. Olsson, P.A.; Hammer, E.C.; Pallon, J.; van Aarle, I.M.; Wallander, H. Elemental composition in vesicles of an arbuscular mycorrhizal fungus, as revealed by PIXE analysis. *Fungal Biol.* **2011**, *115*, 643–648.
39. Hawkes, C.V.; Casper, B.B. Lateral root function and root overlap among mycorrhizal and non mycorrhizal herbs in Florida shrubland, measured using rubidium as a nutrient analog. *Am. J. Bot.* **2002**, *89*, 1289–1294.
40. He, X.; Lilleskov, E. Arsenic Uptake and Phytoremediation Potential by Arbuscular Mycorrhizal Fungi. In *Mycorrhizal fungi: Use in Sustainable Agriculture and Land Restoration*; Solaiman, Z., Abbot, L.K., Varma, A., Eds.; Springer Nature: Berlin/Heidelberg, Germany, 2014; Volume 41, pp. 259–275.
41. Imran, A.; Chaudhry, M.N.; Masood, K.R.; Iqbal, N. Response of sunflower (*Helianthus annuus* L.) to arsenic stress: Accumulation and portioning in different plant parts. *Soil Environ.* **2015**, *34*, 44–50.
42. Burger, A.; Lichtscheidl, I. Strontium in the environment: Review about reactions of plants towards stable and radioactive strontium isotopes. *Sci. Total Environ.* **2019**, *653*, 1458–1512.
43. Hanaka, A.; Dresler, S.; Wójciak-Kosior, M.; Strzemski, M.; Kováčik, J.; Latalski, M.; Zawiślak, G.; Sowa, I. The Impact of Long- and Short-Term Strontium Treatment on Metabolites and Minerals in Glycine max. *Molecules* **2019**, *24*, 3825.

44. Jensen, H.; Gaw, S.; Lehto, N.J.; Hassall, L.; Robinson, B.H. The mobility and plant uptake of gallium and indium, two emerging contaminants associated with electronic waste and other sources. *Chemosphere* **2018**, *209*, 675–684.
45. Yu, X.Z.; Feng, X.H.; Feng, Y.X. Phytotoxicity and Transport of Gallium (Ga) in Rice Seedlings for 2-Day of Exposure. *Bull. Environ. Contam. Toxicol.* **2015**, *95*, 122–125.
46. Seguel, A.; Cumming, J.R.; Klugh-Stewart, K.; Cornejo, P.; Borie, F. The role of arbuscular mycorrhizas in decreasing aluminium phytotoxicity in acidic soils: A review. *Mycorrhiza* **2013**, *23*, 167–183.
47. Coscione, A.R.; Berton, R.S. Barium extraction potential by mustard, sunflower and castor bean. *Sci. Agric.* **2009**, *66*, 59–63.
48. Ubaldini, S.; Guglietta, D.; Vegliò, F.; Giuliano, V. Valorization of Mining Waste by Application of Innovative Thiosulphate Leaching for Gold Recovery. *Metals* **2019**, *9*, 274.